AJNR

CT of parotid tumors.

S Sone, T Higashihara, S Morimoto, J Ikezoe, M Nakatsukasa, J Arisawa and H Tamaki

AJNR Am J Neuroradiol 1982, 3 (2) 143-147
http://www.ajnr.org/content/3/2/143

CT of Parotid Tumors

Shusuke Sone[1]
Tokuro Higashihara[1]
Shizuo Morimoto[1]
Junpei Ikezoe[1]
Mitsuto Nakatsukasa[1]
Jun Arisawa[1]
Hiromitsu Tamaki[2]

Computed tomographic (CT) appearances of 18 surgically proven parotid tumors were studied. Digital radiography (GE, ScoutView) was performed to select the desired gantry angulations and then plain CT and CT combined with sialography were performed. Plain CT clearly showed parotid tumors in nine of the patients. CT combined with sialography was more helpful than plain CT for delineating the tumors in the other patients who had either tumors in high-density parotid glands or tumors of low density. CT allows more accurate evaluation of tumor location and extent in the parotid gland than any other method and helps distinguish malignant from benign lesions. The normal CT appearances of the parotid region are necessary for precise interpretation of CT images in this region.

In evaluating tumors of the parotid region, it is important to know whether they are intrinsic or extrinsic to the parotid gland and to establish the extent of the tumor in relation to the adjacent structures, especially the facial nerve. We recently performed digital radiography (GE, ScoutView) followed by plain computed tomography (CT) and CT combined with sialography for clarification of these diagnostic problems. We briefly describe our technique, discuss the normal CT appearances of the parotid region, especially the appearances of the surrounding muscles, and report a series of 18 patients with parotid tumors on whom CT combined with sialography was performed.

Materials and Methods

Since March 1979, we have examined tumors of the parotid gland using the GE CT/T 8800 scanner. We investigated 18 surgically proven cases, of which 10 were pleomorphic adenomas, five malignant lesions (a case each of mucoepidermoid tumor, adenocarcinoma, undifferentiated carcinoma, acinic cell tumor, and malignant oncocytoma), and three were benign lesions (a case each of Warthin tumor, tubular adenoma, and parotid cyst).

With our technique, a lateral ScoutView image of the skull is obtained initially with two metal markers taped onto the skin; a straight marker is placed along a presumed course of the parotid duct from the tragus to the middle of the upper lip and a second marker outlines the contour of the palpable mass. A selection of CT scan locations is made on this ScoutView on the video display using a movable cursor. The preferable gantry angulation to obtain the full length image of the parotid duct on one slice, and to make additional scans at 1.0 or 1.5 cm intervals parallel to the duct, is determined on the ScoutView by lining up the cursor on the straight marker. The superior and inferior slice locations can be determined by the marker that outlines the mass. When metal dentures interfere with the cursor, another gantry angulation may be used so as to avoid artifacts but to cover the remaining part of the pathologic area (fig. 1). Scans are obtained with a slice thickness of 5 or 10 mm.

In 14 of the 18 patients studied, upon completion of routine CT scanning, parotid CT sialography was performed by cannulating the Stensen duct using a 20 or 27 gauge sialography cannula with an olive tip (Universal Medical Instrument Corp., Ballston Spa, N.Y.). Approximately 8–10 ml of 20% water-soluble contrast medium (a diluted solution of

Received June 9, 1981; accepted after revision October 14, 1981.

Presented at the XVth International Congress of Radiology, Brussels, Belgium, June 1981.

[1] Department of Radiology, Osaka University Medical School, Fukushima-ku, Osaka, 553, Japan. Address reprint requests to S. Sone.

[2] Department of Otorhinolaryngology, Osaka University Medical School, Osaka, Japan.

AJNR 3:143–147, March/April 1982
0195–6108/82/0302–0143 $00.00

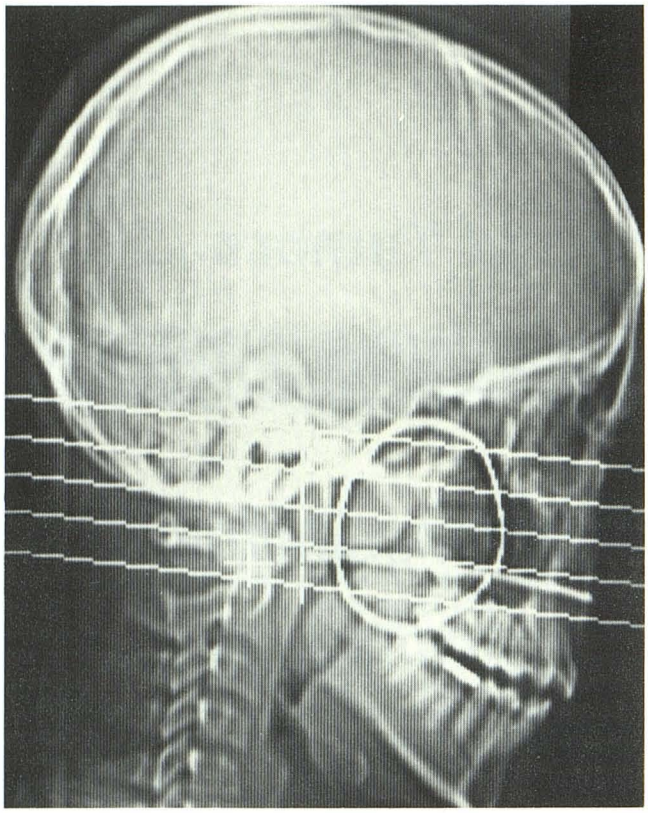

Fig. 1.—Lateral digital film (GE, ScoutView) of skull with two metal markers taped onto skin; one delineates tumor, the other parotid duct. A movable cursor is lined up with straight marker on video display to select desired gantry angulation in order to make contiguous CT images paralleling parotid duct.

65% Angiografin) was injected in order to obtain an adequate parenchymal filling with least discomfort to the patient. However, it should be noted that some of the injected contrast medium occasionally leaked back around the tip of the cannula during injection and also during the subsequent scans. The contrast medium was tolerated without substantial discomfort, but the injection was terminated when the patient felt pain. When Ethiodol from previous conventional sialography, performed either days or weeks before, remained in the parotid tissues and was seen on the CT images, no additional sialography using Angiografin was carried out. In performing conventional sialography before CT scanning, we now avoid the use of Ethiodol when a mass lesion is suspected.

In our series, 14 patients had both plain CT and parotid CT sialography using Angiografin. The other four patients had previous Ethiodol injected and had no further CT sialography using Angiografin. Of 18 patients, CT scans were also obtained during the intravenous infusion of contrast medium in 12.

Anatomy

The parotid gland is seen as a lower density area than the surrounding muscles and a denser area than the fatty tissue on the CT images. The main part of the parotid gland lies immediately below and in front of the external ear posterior to the angle of the jaw. It is partly separated by the facial nerve into superficial and deep parts, which are connected by an isthmus. The superficial part rests anteriorly on the posterior third of the masseter muscle. The posterior part, behind the mandible, extends medially to form the deep retromandibular part, which lies posterior to the pterygoid muscles. The posterior surface of the parotid gland reaches the external acoustic meatus and the mastoid process, inferiorly extends over the sternomastoid muscle and medially over the posterior belly of the digastric muscle and the transverse process of the atlas. The posteromedial aspect of the parotid gland rests on the styloid process and the three muscles (the stylohyoid, the styloglossus,

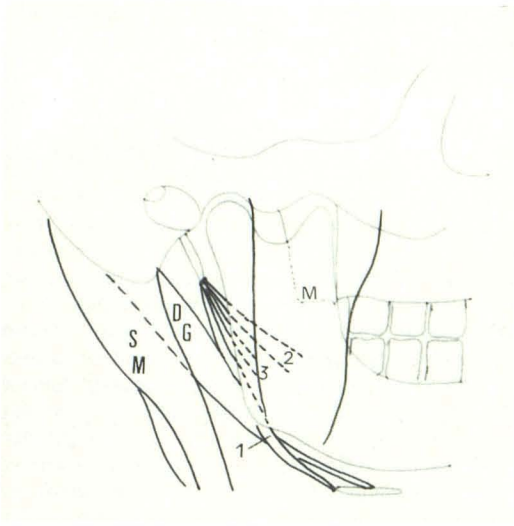

2

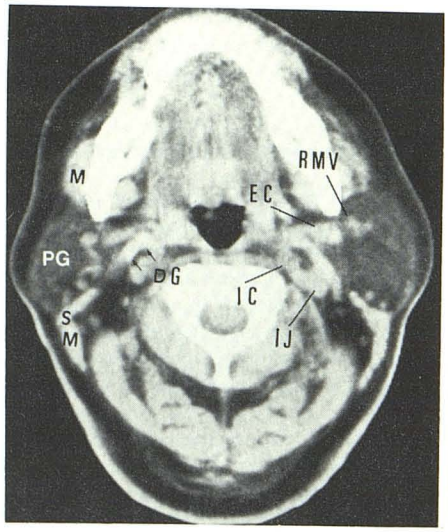

3

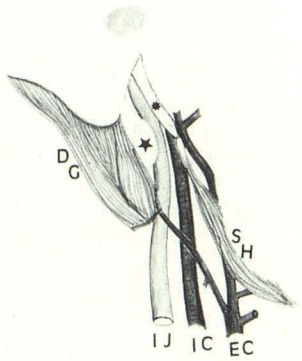

4

Fig. 2.—Musculatures deep to parotid bed, lateral view. M = masseter, SM = sternomastoid, DG = digastric, 1 = stylohyoid, 2 = styloglossus, 3 = stylopharyngeus. Medial and lateral pterygoids running from pterygoid plate to ramus of mandible are omitted.

Fig. 3.—Normal CT of parotid region. PG = parotid gland, M = masseter, SM = sternomastoid, DG = digastric, RMV = retromandibular vein, EC = external carotid artery, IC = internal carotid artery, IJ = internal jugular vein.

Fig. 4.—Vessels deep to parotid bed, lateral view. EC = external carotid artery, IC = internal carotid artery, IJ = internal jugular vein, DG = digastric muscle, SH = stylohyoid muscle, asterisk = styloid process, star = transverse process of atlas.

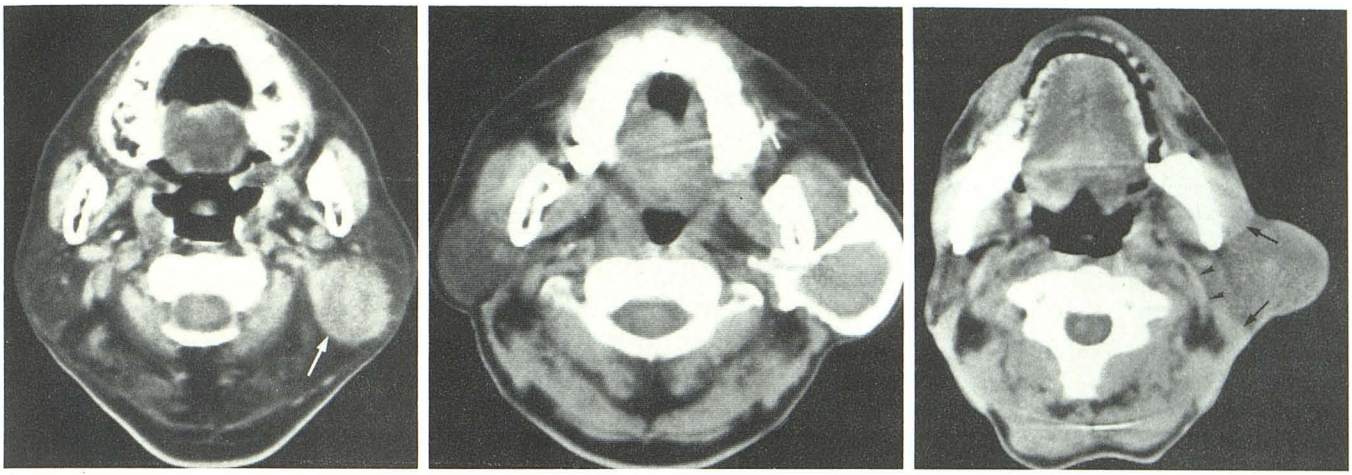

A B C

Fig. 5.—CT appearances of parotid tumors. **A**, Pleomorphic adenoma with slightly irregular margin in posteroinferior part of left parotid gland. On plain CT, mass (*arrow*) in low density parotid tissue is clearly shown. **B**, Warthin tumor in superficial part of left parotid gland. Slightly lobulated margin of tumor on CT sialogram. Mass displaces masseter muscle forward and sternomastoid muscle backward. Normal filling of deep part of parotid gland. **C**, Adenocarcinoma of left parotid. Mass with indistinct margins displaces masseter muscle forward and sternomastoid muscle backward (*arrows*). Digastric muscle also slightly displaced medially (*arrowheads*).

and the stylopharyngeus muscles) that are attached to it, and, more anteriorly, the gland extends toward the parapharyngeal space (figs. 2 and 3) [1–3].

The internal jugular vein, internal carotid artery, and the last four cranial nerves pass deeply to the digastric muscle and the styloid process. The external carotid artery is separated from the internal carotid artery by the styloid process in the upper part of the neck (fig. 4) [1].

The parotid duct takes a course between the tragus and the middle part of the upper lip. At the anterior border of the masseter muscle, it turns medially and opens on the mucosal surface of the cheek [2].

The facial nerve descends from the stylomastoid foramen, runs in front of the digastric muscle and lateral to the styloid process, and enters the parotid gland. Within the gland, it takes a forward course and becomes more superficial. It then divides into peripheral branches and lies superficial to the retromandibular vein [1, 2]. The origin of the posterior belly of the digastric muscle lies posterior to the facial nerve. The more distal part of the posterior part of the digastric muscle is medial to the nerve. The retromandibular vein is usually located medial to and is crossed by the facial nerve. Therefore, the locations of the posterior belly of the digastric muscle and the retromandibular vein provide landmarks for the estimation of the course of the nerve.

Results

The density of the parotid gland on the CT images varies considerably from patient to patient. It ranges between a slightly higher density than the fatty tissue to a slightly lower density than the muscle. The parotid gland of the uninvolved side showed a low density (slightly denser than the fatty tissue) in nine of the 18 patients in this series, intermediate density in three patients, and a relatively high density (slightly less dense than the muscule) in six patients. No definite relation was observed between the density of the parotid gland and the patient's advancing age. The factors associated with the variable density of the gland need to be studied further.

Parotid tumors usually showed a slightly higher attenuation value than the gland. They may easily be seen when the density of the surrounding normal gland tissue is low, but not when the density is high. In six of the nine patients with low density parotid glands, the parotid tumors were clearly shown. In the other three patients (two with pleomorphic adenomas and one with a tubular adenoma), the tumors were faintly shown due to the low density of the tumor itself. In two of the three patients with intermediate density parotid glands, the tumors were easily recognized, and, in the other patient with a parotid cyst, the margin of the mass could not be well delineated on the plain CT images, probably due to the low CT density of the mass (23 Hounsfield units). The cyst became clearly outlined on the intravenous postenhancement CT scan because of the enhancement of the surrounding normal parotid gland. In five of the six patients with relatively high density parotid glands, the mass could not be identified in the enlarged glands. In the other patient with an oxyphilic adenoma, identification of the mass was not difficult because the mass was huge with an irregular margin and a density higher than the parotid gland and approximately equal to the muscle tissue.

There were 10 patients with pleomorphic adenomas. Of these, nine patients had plain CT scanning and one had only CT after sialography. One of the nine adenomas demonstrated a smooth and sharply marginated mass. Five showed a slightly irregular outline (fig. 5A). The margins of the adenomas in the other three patients, who had relatively dense parotid glands, were rather indistinct. The Warthin tumor showed a moderately lobulated margin (fig. 5B). In all five patients with malignant lesions, irregular or poorly defined margins of the tumors were shown (fig. 5C).

The lesions located posteriorly in the gland displaced the

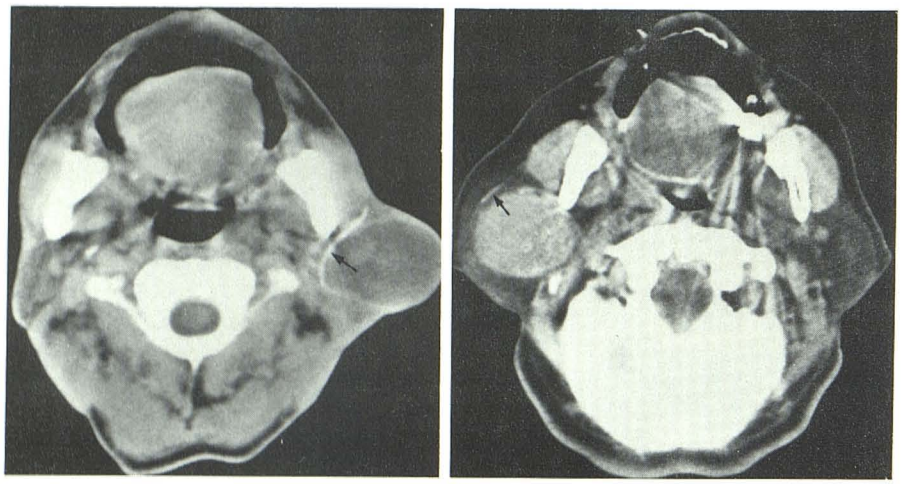

Fig. 6.—Displacement of parotid duct on parotid CT sialography. **A**, (Same case as in fig. 5C.) Medially displaced main duct (*arrow*) suggests tumor arises from superficial lobe. Poor parenchymal filling because of painful injection. **B**, Pleomorphic adenoma. Mass with slightly irregular margin. Lateral displacement of parotid duct (*arrow*) suggests tumor arises from deep lobe. Poor parenchymal filling because of leakage of contrast into oral cavity.

sternomastoid muscle posteriorly and the posterior belly of the digastric posteromedially. Anterior lesions displaced the posterior part of the masseter muscle anteriorly. The tumors with retropharyngeal extension passed through the stylomandibular tunnel and occupied the space between the medial pterygoid muscle and the stylomandibular ligament, the styloid process, and the three muscles attached to the process. The low density fatty area surrounding these muscles and the major vessels that lie medial to the styloid process became narrowed or indistinct. Comparing these structures with those on the opposite side helped to detect a minor abnormality.

Involvement of the facial nerve by a parotid tumor could be predicted with a high degree of confidence when the tumor occupied an upper part of the gland, intimately associated with the tip of the mastoid and the stylomastoid foramen. When the tumor was located in a lower part of the gland, the retromandibular vein was used to evaluate the relation of the tumors to the facial nerves.

CT combined with sialography showed the course of the Stensen duct and its major branches, and the parenchymal filling of the parotid gland after a sufficient amount of contrast medium had been injected. This method was useful in showing the size and extent of the parotid tumor not clearly identified on plain CT because the tumor was located in a parotid gland of a relatively high density. The site of origin of the tumor within the parotid gland could be determined by the position of the filling defects in the parotid parenchyma (fig. 5B) and/or by the displacement of the main ducts laterally or medially (fig. 6). The tumors arising from the superficial lobe displaced the main duct medially and/or showed normal parenchymal filling deep to the mass. The tumors in the deeper part displaced the duct laterally and/or the parenchymal filling superficial to the mass was obtained. Posterior lesions did not affect the main ducts.

Discussion

The usefulness of CT for the evaluation of the parotid tumors has been reported. Parotid CT sialography has been used to obtain more precise mapping than plain CT can provide imaging of the gland's parenchyma and of tumor filling defects [4–8].

In nine patients in our series, the parotid tumors were clearly seen on plain CT images and almost all of them had relatively high density contrasting the low density parotid gland. In the other nine patients, the tumor could not be clearly identified on the plain CT images because of the high density of the surrounding parotid glands or due to the low density of the tumor itself. For these patients, CT combined with sialography was valuable to delineate filling defects within the glands.

Our technique using a ScoutView localization radiograph permits easy selection of CT scan locations to obtain the full length image of the parotid duct on one slice and with the other slices effectively covering the tumor. The image of the parotid duct thus obtained provides additional information concerning the tumor location. CT combined with sialography can determine, by lateral or medial displacement of the main ducts, the site of origin of any tumor located near the junction of the superficial and deep lobes. When a tumor was clearly shown on CT images, CT combined with sialography was not required, especially for posteriorly located tumors because these tumors usually do not affect the main ducts.

CT was helpful in distinguishing malignant from benign lesions. Irregular or poorly defined margins suggested malignancy and smooth or slightly irregular margins benignity. In estimating extension of the tumor, displacement or deformity of the muscles such as the masseter, the sternomastoid, and the posterior belly of the digastric was one of the most important findings. Facial nerve involvement could be predicted using the mastoid tip and styloid process for superior tumors and the retromandibular vein for inferior tumors.

CT during intravenous infusion of contrast medium was useful only in the case of the parotid cyst, which was clearly delineated as a lower density area within the contrast-enhanced normal gland tissue. In other patients with parotid tumors, however, little additional important information was obtained after intravenous contrast administration.

ACKNOWLEDGMENT

We thank Satoko Matsuura for assistance in manuscript preparation.

REFERENCES

1. Boileau Grant JC. *Grant's atlas of anatomy*, 5th ed. Baltimore: Williams & Wilkins, **1966**:540–552, 572–574
2. Rankow RM, Polayes IM. Surgical treatment of salivary gland tumors. In: *Diseases of the salivary glands*. Philadelphia: Saunders, **1976**:156–161, 239–250
3. Fluur E. Parapharyngeal tumors. *Arch Otolaryngol* **1964**; 80:557–565
4. Carter BL, Karmody CS. Computed tomography of the face and neck. *Semin Roentgenol* **1978**;13:257–266
5. Mancuso AA, Rice D, Hanafee W. Computed tomography of the parotid gland during contrast sialography. *Radiology* **1979**;132:211–213
6. Som PM, Biller HF. The combined CT-sialogram. *Radiology* **1980**;135:387–390
7. Mancuso AA, Bohman L, Hanafee W, Maxwell D. Computed tomography of the nasopharynx: normal and variants of normal. *Radiology* **1980**;137:113–121
8. Stone DN, Mancuso AA, Rice D, Hanafee WN. Parotid CT sialography. *Radiology* **1981**;138:393–397